

Copper supplementation alleviates hypoxia-induced ferroptosis and oxidative stress in neuronal cells

JIANYU WANG^{1,2*}, YUANKANG ZOU^{1*}, RUILI GUAN^{1*}, SHUANGSHUANG TAN^{1,3}, LIHONG SU^{1,3},
ZAIHUA ZHAO¹, ZIPENG CAO¹, KUNYAN JIANG¹, TAO WANG¹ and GANG ZHENG¹

¹Department of Occupational and Environmental Health and The Ministry-of-Education's Key Laboratory of Hazard Assessment and Control in Special Operational Environment, School of Preventive Medicine, Fourth Military Medical University, Xi'an, Shaanxi 710032, P.R. China; ²Department of Radiation Protection Medicine, School of Preventive Medicine, Fourth Military Medical University, Xi'an, Shaanxi 710032, P.R. China; ³School of Public Health, Gansu University of Chinese Medicine, Lanzhou, Gansu 730000, P.R. China

Received March 7, 2024; Accepted September 18, 2024

DOI: 10.3892/ijmm.2024.5441

Abstract. Hypoxic ischemia is the primary cause of brain damage in newborns. Notably, copper supplementation has potential benefits in ischemic brain damage; however, the precise mechanisms underlying this protective effect remain unclear. In the present study, a hypoxic HT22 cell model was developed to examine the mechanism by which copper mitigates hypoxia-induced oxidative stress. Cell viability was assessed using the Cell Counting Kit-8 assay, mitochondrial structure was examined with a transmission electron microscope, intracellular ferrous ions and lipid reactive oxygen species levels in HT22 cells were measured using FerroOrange and BODIPY 581/591 C11 staining, copper content was determined using graphite furnace atomic absorption spectroscopy, and gene and protein expression were analyzed by reverse transcription-quantitative PCR and western blotting. The present findings indicated that hypoxic exposure may lead to reduced cell viability, along with the upregulation of various markers associated with ferroptosis. Furthermore, hypoxia elevated the levels of reactive oxygen species, hydrogen peroxide and malondialdehyde, and decreased the activity of superoxide dismutase 1 (SOD1) in HT22 cells. In addition, the intracellular copper concentration exhibited a notable decrease, while supplementation with an appropriate dose of copper effectively shielded neurons from hypoxia-induced

oxidative stress and ferroptosis, and elevated cell viability in hypoxia-exposed HT22 cells through the copper chaperone for superoxide dismutase/SOD1/glutathione peroxidase 4 axis. In conclusion, the present study identified a novel function of copper in protecting neurons from oxidative stress and ferroptosis under hypoxic conditions, providing fresh insights into the therapeutic potential of copper in mitigating hypoxia-induced neuronal injury.

Introduction

Neonatal hypoxic-ischemic brain damage is caused by perinatal asphyxia. The incidence of hypoxic-ischemic brain damage in developed countries is estimated to be 1-8% for new births every year (1,2). Currently, mild therapeutic hypothermia is used to cure perinatal asphyxia and to reduce the damage caused by hypoxic brain damage (3). Children with severe perinatal asphyxia may experience notable complications, such as severe hypoxic ischemic organ damage, which can have long-lasting effects on their future health and wellbeing (4).

Neuronal cell death is the main pathophysiological alteration that occurs after hypoxic brain damage and contributes to long-term neurological disorders. Previous studies have shown that hypoxic brain damage induces a serious form of cell death that occurs concurrently or sequentially (5,6). Cerebral hypoxia has been reported to rapidly elevate the levels of reactive oxygen species (ROS), leading to the direct modification of cellular macromolecules, such as cell membranes, lipids and DNA. Consequently, oxidative stress and inflammatory responses are induced (7). Ferroptosis, a form of cell death driven by peroxidation, is associated with hypoxic brain damage. Lin *et al* (8) observed elevated iron levels in the brain tissues of neonatal patients with hypoxic brain damage. Additionally, the modulation of iron metabolism through the use of desferrioxamine and erythropoietin may potentially improve the prognosis of hypoxic brain damage (9).

Numerous critical brain processes rely on copper, an essential trace element, as evidenced by various studies (10-12). Studies on patients with ischemic stroke have shown an increase in plasma copper concentrations (13,14), indicating

Correspondence to: Dr Gang Zheng or Dr Tao Wang, Department of Occupational and Environmental Health and The Ministry-of-Education's Key Laboratory of Hazard Assessment and Control in Special Operational Environment, School of Preventive Medicine, Fourth Military Medical University, 169 Changlexi Road, Xi'an, Shaanxi 710032, P.R. China
E-mail: zhenggang@fmmu.edu.cn
E-mail: taowang@fmmu.edu.cn

*Contributed equally

Key words: hypoxia, neurons, copper, ferroptosis, oxidative stress

copper dyshomeostasis following hypoxic-ischemic brain damage. Previous studies have demonstrated the protective effects of supplemental copper against ischemic brain injury (15,16); however, the precise mechanism by which copper supplementation affects hypoxia-induced brain damage remains unclear. Copper serves as the catalytic center for antioxidant enzymes. Previous studies have shown that copper secretion can protect cells from ferroptosis (17,18), suggesting that supplementation with copper could have beneficial effects on ferroptosis-induced cell death. The aim of the present study was to evaluate the effects of copper supplementation on hypoxia-induced neuronal damage and ferroptosis. The current study may offer valuable insights into a therapeutic approach for hypoxia-induced cellular damage by utilizing copper supplementation.

Materials and methods

Materials. Copper dichloride (CuCl_2) was purchased from MilliporeSigma. Anti-copper transporting α polypeptide (ATP7A) (cat. no. PA5-103110), anti-copper transporting β polypeptide (ATP7B) (cat. no. PA1-16583), anti-copper transporter 1 (CTR1) (cat. no. PA1-16586) and BODIPYTM 581/591 C11 (cat. no. D3861) were purchased from Invitrogen (Thermo Fisher Scientific, Inc.). Anti-copper chaperone for superoxide dismutase (CCS) (cat. no. ab167170), anti-superoxide dismutase (SOD)1 (cat. no. ab51254), anti- β actin (cat. no. ab6276), Goat Anti-Rabbit IgG H&L (HRP) (cat. no. ab205718) and Goat Anti-Mouse IgG H&L (HRP) (cat. no. ab205719) were purchased from Abcam. Anti-XIAP (cat. no. 2042S) and anti-glutathione peroxidase 4 (GPX4) (cat. no. 52455S) were purchased from Cell Signaling Technology, Inc. The Cell Counting Kit (CCK)-8 assay kit was purchased from APeXBio Technology LLC. Ferrostatin-1 (Fer-1; cat. no. HY-100579) was purchased from MedChemExpress and FerroOrange (cat. no. F374) was purchased from Dojindo Laboratories, Inc. ROS (cat. no. S0033S), malondialdehyde (MDA; cat. no. S0131S), hydrogen peroxide (H_2O_2 ; cat. no. S0038) and Cu/Zn-SOD and Mn-SOD Assay Kit with WST-8 (cat. no. S0103) kits were purchased from Beyotime Institute of Biotechnology.

Cell culture and exposure to hypoxia. HT22 mouse hippocampal neuronal cells were procured from the American Type Culture Collection. Following resuscitation, the cells were cultured in high-glucose DMEM (Gibco; Thermo Fisher Scientific, Inc.) supplemented with 10% fetal bovine serum (Gibco; Thermo Fisher Scientific, Inc.), 1% streptomycin and 1% penicillin at 37°C with 5% CO_2 .

A microaerophilic incubation system (DWS-H85; Don Whitley Scientific Limited) filled with 1% O_2 and 5% CO_2 was used to generate an *in vitro* model of hypoxic exposure for 48 h, as described previously (19). The culture medium was pre-treated in the microaerophilic incubation system for 9 h before use.

For Fer-1 and copper treatment, HT22 cells were cultured with media containing 1 μM Fer-1 and 5 μM CuCl_2 for 48 h at 37°C.

CCK-8 analysis. The CCK-8 assay kit was used to determine the effects of a hypoxic challenge on cell viability. This kit uses a water-soluble tetrazolium salt to quantify the number

of live cells by producing an orange formazan dye upon bioreduction in the presence of an electron carrier. HT22 cells (8×10^3 cells/well) were incubated for 24 h in a 96-well plate. Following exposure to hypoxic conditions (12, 24, 36, 48 and 72 h), 10 μl CCK-8 reagent was added and the cells were then incubated for 2 h at 37°C. Finally, the optical density (OD) was measured at 450 nm. Cell viability was calculated as follows: (OD value of experimental groups - OD value of blank groups) / (OD value of control groups - OD value of blank groups).

Transmission electron microscopy (TEM). After 48 h of exposure to hypoxia, HT22 cells were collected, prefixed in 2.5% glutaraldehyde phosphate (0.1 M, pH 7.4) overnight at 4°C, and postfixed in 2% buffered osmium tetroxide at 4°C for 15 min. The fixed cells were dehydrated with 70, 80, 90 and 100% ethanol (each for 15 min). Subsequently, the cells were embedded in Epon812 (Merck KGaA) at room temperature for 30 min, and ultrathin sections (60 nm) were cut and stained with uranyl acetate and lead citrate at room temperature for 30 min. Images were captured using TEM (FEI; Thermo Fisher Scientific, Inc.).

Western blot analysis. A lysis buffer (RIPA Lysis Buffer; cat. no. P0013C; Beyotime Institute of Biotechnology) containing protease inhibitors was used to extract proteins from HT22 cells and western blotting was performed to detect protein expression. After protein extraction, the BCA detection kit (cat. no. 23225; Thermo Fisher Scientific, Inc.) was used to quantify the protein concentration. Protein samples (30 μg) were then subjected to sodium dodecyl sulfate-polyacrylamide gel electrophoresis on 10% gels and were transferred onto polyvinylidene difluoride membranes, which were incubated in 5% bovine serum albumin (cat. no. ST023; Beyotime Institute of Biotechnology) at room temperature for 1 h. Subsequently, the membranes were incubated with primary antibodies at 4°C overnight (anti-ATP7A, 1:1,000; anti-ATP7B, 1:1,000; anti-CTR1, 1:500; anti-CCS, 1:1,000; anti-SOD1, 1:1,000; anti-XIAP, 1:1,000; anti-GPX4, 1:1,000; anti- β -actin, 1:1,000). The membranes were then washed three times with Tris-buffered saline-0.1% Tween 20, and were incubated with the corresponding horseradish peroxidase-conjugated antibodies (Anti-Rabbit IgG antibody, 1:500; Anti-Mouse IgG antibody, 1:500) for 2 h at room temperature. A chemiluminescence system (Bio-Rad Laboratories, Inc.) was used to visualize the protein bands. After being normalized to β -actin, ImageJ (version 1.51; National Institutes of Health) was adopted to evaluate the protein expression; protein expression levels were normalized to those in control cells.

ROS levels. Intracellular ROS levels were measured using a ROS assay kit. HT22 cells (2×10^7) were collected after 48 h of exposure to hypoxia, were resuspended in 2 ml DMEM and were incubated with 10 μM DCFH-DA for 20 min at 37°C. Finally, the cells were measured at 488 nm excitation and 525 nm emission using a fluorescence spectrophotometer (BioTek; Agilent Technologies, Inc.). The relative ROS content was normalized to the number of cells.

H₂O₂ levels. HT22 cells were collected after being exposed to hypoxia (1% O₂) for 48 h. H₂O₂ levels were detected using an assay kit. Briefly, a standard curve was constructed using standard H₂O₂ solutions and the corresponding OD values. HT22 cells were prepared using RIPA lysis buffer (cat. no. P0013C; Beyotime Institute of Biotechnology) and the corresponding OD values were detected at 520 nm. Accurate H₂O₂ levels were calculated using the standard curve.

MDA, SOD and SOD1 assays. A MDA assay kit was used to quantify the generation of MDA, whereas a Cu/Zn-SOD and Mn-SOD assay kit (cat. no. S0103; Beyotime Institute of Biotechnology) was used to measure the levels of SOD and SOD1 enzyme activity. Briefly, HT22 cells were trypsinized according to the manufacturer's instructions. After sonication (20 kHz) was carried out in five 1-min cycles on ice (30-sec sonication and 30-sec rest), the lysed cells were centrifuged at 16,114 x g for 15 min at 4°C to remove the debris. The total protein, and MDA, SOD and SOD1 levels in the supernatant were measured and normalized to mg protein, according to the manufacturer's protocols.

Copper concentration. The intracellular copper concentration in HT22 cells was measured using graphite furnace atomic absorption spectroscopy (GF-ASS). Briefly, HT22 cells were exposed to hypoxia for 24 and 48 h, after which, the medium was refreshed with complete medium containing 5 μM CuCl₂ for 5 h at 37°C in an incubator. Subsequently, the cells were cultured and centrifuged at 6,500 x g for 10 min to obtain cell clumps, which were then dried and weighed, followed by incubation with 100 μl nitric acid at 100°C for 1 h for nitrolysis, and then the cell digestion solution (40 μl) was mixed with 360 μl diluent (1% nitric acid + 0.1% Triton + 98.9% ddH₂O), and subsequently, 20 μl of the resulting mixture was introduced into the GF-ASS (PinAAcle900T; PerkinElmer, Inc.) for the detection of copper. Finally, the copper concentration in HT22 cells was normalized to the sample weight.

Intracellular ferrous ions and lipid reactive oxygen species (LOS). The fluorescence levels of total intracellular ferrous ions and LOS in HT22 cells were detected using FerroOrange and BODIPY 581/591 C11 respectively. After treatment with 5 μM CuCl₂ at 37°C for 48 h, cells in confocal dishes were resuspended in 2 ml fresh Hank's balanced salt solution (cat. no. PB180323; Procell Life Science & Technology Co., Ltd.). The cells were then incubated with 1 μM C11-BODIPY or FerroOrange for 20 min at 37°C. After two washes, intracellular FerroOrange and C11-BODIPY (581/591) fluorescence imaging was performed using a fluorescence microscope. The maximum absorbance of excitation and emission wavelengths of FerroOrange is 543/580 nm, and that of C11-BODIPY (581/591) is 488/510 nm. The images were analyzed using ImageJ.

Small interfering RNA (siRNA) transfection. For siRNA-induced knockdown, CCS siRNA and a normal control (NC) siRNA were designed and synthesized by Shanghai GenePharma Co., Ltd. The sequences were as follows: CCS siRNA, forward (F) 5'-GGUAUGGGCAGUAGCCAAUTT-3', reverse (R) 5'-AUUGGCUACUGCCCAUACCTT-3';

NC siRNA, 5'-F UUCUCCGAACGUGUCACGUTT-3' and R 5'-ACGUGACACGUUCGGAGAATT-3'. Cells (1x10⁷) were transiently transfected with 400 nM siRNA using 1% Lipofectamine[®] 2000 (cat. no. 11668030; Invitrogen; Thermo Fisher Scientific, Inc.) in Opti-MEM (cat. no. 31985070; Invitrogen; Thermo Fisher Scientific, Inc.) according to the manufacturer's instructions. After 6 h of incubation at 37°C, the medium was replaced and other experiments were conducted 8 h later. Transfection efficiency was measured using western blot analysis.

RNA extraction and reverse transcription-quantitative (q)PCR. According to the manufacturer's instructions, total RNA was isolated from cells using TRIzol[®] reagent (cat. no. 15596018; Invitrogen; Thermo Fisher Scientific, Inc.) and was then reverse transcribed into cDNA using PrimeScript Master Mix (cat. no. RR036A; Takara Biotechnology Co., Ltd.) according to the manufacturer's protocol (37°C for 15 min and 85°C for 5 sec). qPCR was performed using TB Green Premix Ex Taq II (cat. no. RR820A; Takara Biotechnology Co., Ltd.) on an Applied Biosystems QuantStudio 5 instrument (Applied Biosystems; Thermo Fisher Scientific, Inc.), and the qPCR thermocycling conditions were as follows: 95°C for 30 sec, followed by 40 cycles at 95°C for 30 sec and 60°C for 34 sec. Quantification of qPCR data was performed using the 2^{-ΔΔC_q} method (20). All data were normalized to the expression levels of β-actin. The specific primers used were as follows: GPX4, F 5'-GATGGAGCCCATTCCTGAACC-3', R 5'-CCC TGTACTTATCCAGGCAGA-3'; β-actin, F 5'-GGCTGTATT CCCCTCCATCG-3' and R 5'-CCAGTTGGTAACAATGCC ATGT-3'.

Cell apoptosis assay. Apoptosis was detected by flow cytometry using an Annexin V-FITC kit (cat. no. C1062S; Beyotime Institute of Biotechnology). According to the manufacturer's instructions, after 48 h of exposure to hypoxia, HT22 cells were harvested via centrifugation (1,000 x g, 5 min) at room temperature and resuspended in Annexin V-FITC binding solution. Subsequently, the samples were mixed with Annexin V-FITC staining solution, followed by PI staining solution. The mixture was then incubated at room temperature for 20 min and analyzed using a CytoFLEX flow cytometer (Beckman Coulter, Inc.). CytExpert 2.4 software (Beckman Coulter, Inc.) was used for data analysis.

Statistical analysis. All experiments were conducted in triplicate and all data were analyzed using GraphPad Prism 9 (Dotmatics). Data are presented as the mean ± SEM. One-way ANOVA was performed to compare more than two groups followed by Tukey's post hoc test, whereas unpaired Student's t-test was used to compare the differences between two groups. P<0.05 was considered to indicate a statistically significant difference.

Results

Hypoxia induces ferroptosis in neurons. The CCK-8 assay was performed on HT22 cells after exposure to hypoxia for 12, 24, 36, 48 and 72 h to assess the impact of hypoxia on neurons. The results indicated that the viability of HT22 cells was notably

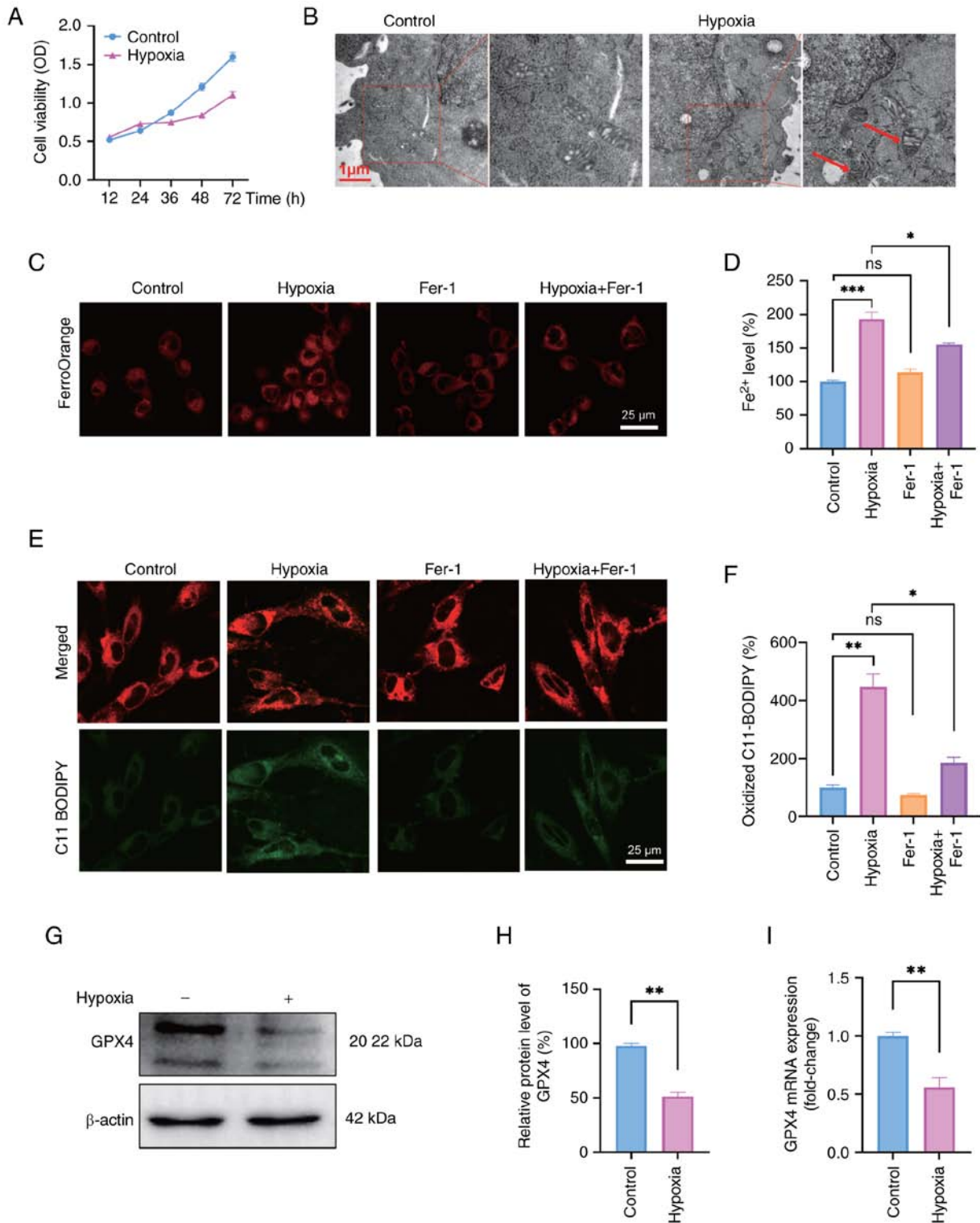


Figure 1. Hypoxia induces ferroptosis in neurons. (A) HT22 cell viability at different time points was detected by Cell Counting Kit-8 assay. (B) Images of the ultrastructure of mitochondria in HT22 cells exposed to normoxia and hypoxia (1% O₂) for 48 h were captured under a transmission electron microscope. Red arrows indicate shrunken mitochondria. Scale bars, 1 μ m. (C) Ferrous ion levels detected by FerroOrange staining and (D) corresponding semi-quantification by ImageJ. Scale bars, 25 μ m. (E) Lipid reactive oxygen species staining with the fluorescent probe C11-BODIPY and (F) corresponding semi-quantification. Scale bars, 25 μ m. (G) Western blot analysis and (H) semi-quantification of the protein expression levels of the ferroptosis biomarker GPX4 following exposure of cells to hypoxia for 48 h. (I) mRNA expression levels of GPX4 after exposure to hypoxia for 48 h. One-way ANOVA was used for multiple-group comparisons, and unpaired Student's t-test for two-group comparisons. Data are presented as the mean \pm SEM (n=3). *P<0.05, **P<0.01, ***P<0.001. Fer-1, ferrostatin-1; GPX4, glutathione peroxidase 4; ns, not significant; OD, optical density.

slower following hypoxic exposure compared with that of the control group, suggesting potential damage to the cells caused by hypoxia (Fig. 1A). Additionally, TEM analysis revealed

distinctive morphological changes in HT22 cells exposed to hypoxia for 48 h, including smaller mitochondria and increased membrane density (Fig. 1B). FerroOrange staining

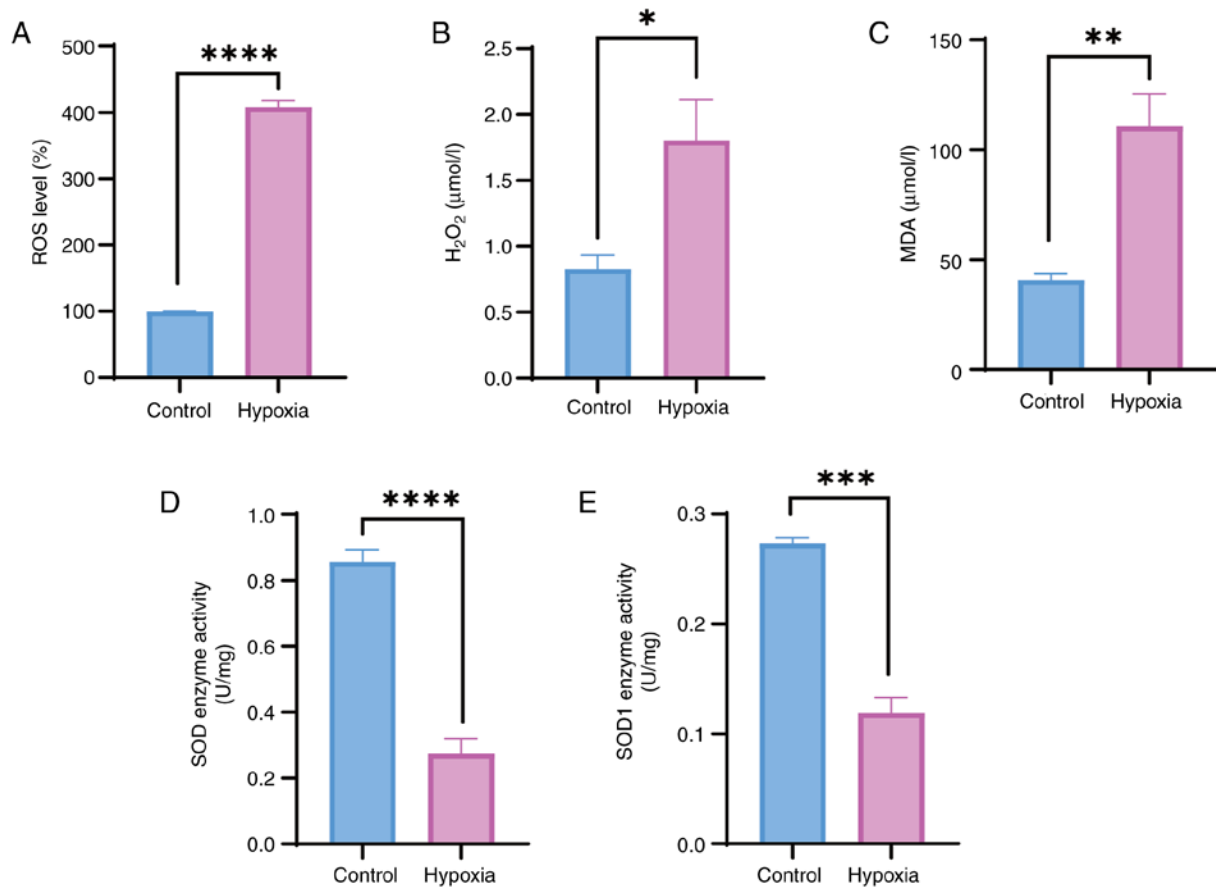


Figure 2. Hypoxia leads to oxidative stress in neurons. Detection of (A) ROS levels, (B) H₂O₂, (C) MDA, and (D) SOD and (E) SOD1 enzyme activity in HT22 cells exposed to normoxia or hypoxia (1% O₂) for 48 h. Unpaired Student's t-test was used for analysis. Data are presented as the mean ± SEM (n=3). *P<0.05, **P<0.01, ***P<0.001, ****P<0.0001. H₂O₂, hydrogen peroxide; MDA, malondialdehyde; ns, not significant; ROS, reactive oxygen species; SOD, superoxide dismutase.

showed that cells subjected to hypoxia exhibited notable accumulation of ferrous ions. This effect was attenuated by administering Fer-1, as evidenced by a reduction in ferrous ion staining (Fig. 1C and D). Increased levels of ferrous ions induce oxidative stress, particularly LOS, thereby indicating that ferroptosis may serve a potential role in the pathogenesis of hypoxia. As expected, increased LOS levels were detected in HT22 cells exposed to hypoxia using the fluorescent probe C11-BODIPY, whereas a substantial decrease in LOS accumulation was observed when the cells were exposed to hypoxia with Fer-1 treatment (Fig. 1E and F). The expression levels of GPX4 were detected as a marker of ferroptosis to provide additional evidence of hypoxia-induced ferroptosis in HT22 cells. The results revealed a significant decrease in the protein expression levels of GPX4 in HT22 cells subjected to hypoxia compared with those in the control group (Fig. 1G and H). In addition, the alteration in the mRNA expression levels of GPX4 was consistent with that in the protein levels (Fig. 1I). Additionally, the present study measured apoptotic cells using an Annexin V-FITC/PI apoptosis detection kit; the results indicated a slight but insignificant increase in apoptosis following 48 h of exposure to hypoxia (Fig. S1). These findings suggested that hypoxia may induce ferroptosis and potentially intensify oxidative stress.

Neurons are subjected to oxidative stress under hypoxia. The intracellular ROS levels were measured after exposure to

hypoxia for 48 h to investigate the effects of hypoxia on oxidative stress in HT22 cells. These results indicated a significant increase in intracellular ROS levels (Fig. 2A). H₂O₂ levels were also significantly increased in HT22 cells following exposure to hypoxia for 48 h (Fig. 2B). Furthermore, MDA, a final product of polyunsaturated fatty acid peroxidation and a marker of oxidative stress, was measured in HT22 cells and was significantly increased in response to hypoxia compared with that in the control group (Fig. 2C). SOD serves an essential role in the first line of antioxidant defense. The present study examined the activities of SOD and SOD1 enzymes in HT22 cells, and revealed that their activities were markedly reduced in the hypoxia group compared with those in the control group (Fig. 2D and E). These results suggested that hypoxia may weaken the overall antioxidant capacity of neurons.

HT22 cells exposed to hypoxic conditions exhibit abnormal copper metabolism. The copper concentration in HT22 cells exposed to hypoxia for 24 and 48 h was quantified to investigate the impact of hypoxia on the copper metabolism of HT22 cells. The results indicated a significant decrease in the copper concentration after both 24 and 48 h of exposure to hypoxia (Fig. 3A). The expression levels of four copper transport proteins, namely, CTR1, ATP7A, ATP7B and CCS, were assessed to further elucidate the mechanisms underlying this alteration in intracellular copper concentration. Western blot analysis indicated that the expression levels of ATP7B,

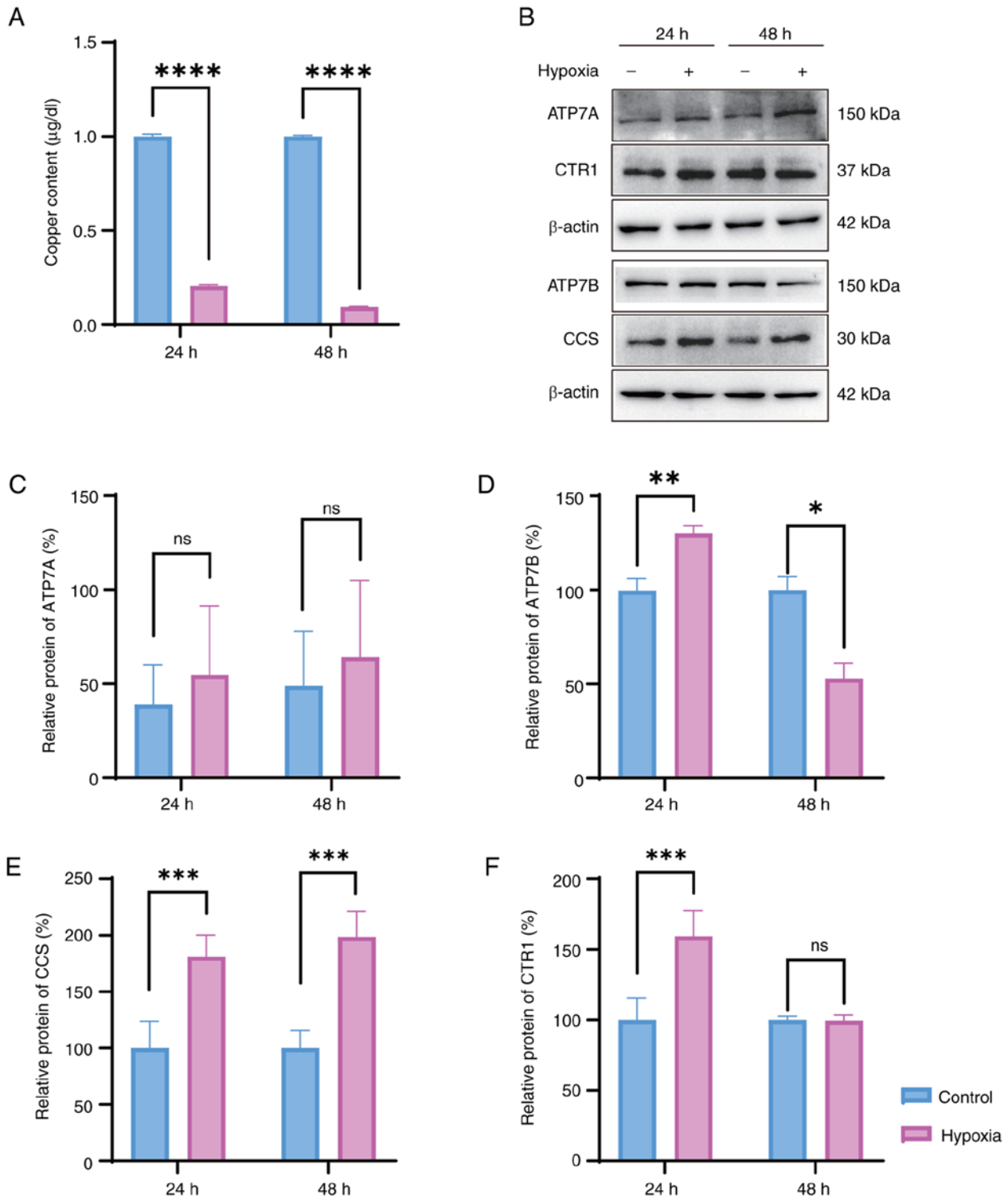


Figure 3. Copper metabolism is involved in the survival of HT22 cells exposed to hypoxia. (A) Copper content of HT22 cells exposed to hypoxia for 24 and 48 h, as determined by graphite furnace atomic absorption spectroscopy. (B) Western blot analysis and semi-quantification of the protein expression levels of copper transport proteins, including (C) ATP7A, (D) ATP7B, (E) CCS and (F) CTR1 was determined following exposure to hypoxia (1% O₂) for 24 and 48 h. Unpaired Student's t-test was used for analysis. Data are presented as the mean ± SEM (n=3). *P<0.05, **P<0.01, ***P<0.001, ****P<0.0001. ATP7A, copper transporting α polypeptide; ATP7B, copper transporting β polypeptide; CCS, copper chaperone for superoxide dismutase; CTR1, copper transporter 1; ns, not significant.

CTR1 and CCS were elevated after 24 h of hypoxic exposure compared with those in the control group, whereas the expression of ATP7A showed no significant difference (Fig. 3B-F). However, as the duration of hypoxic exposure increased, the expression levels of ATP7B decreased, and the expression

of CTR1 remained relatively stable after 48 h of hypoxia compared to that in the control group (Fig. 3B-F). These results suggested distinct copper levels and copper transporter alterations following exposure to hypoxia, potentially implicating alterations in hypoxia-induced cell damage.

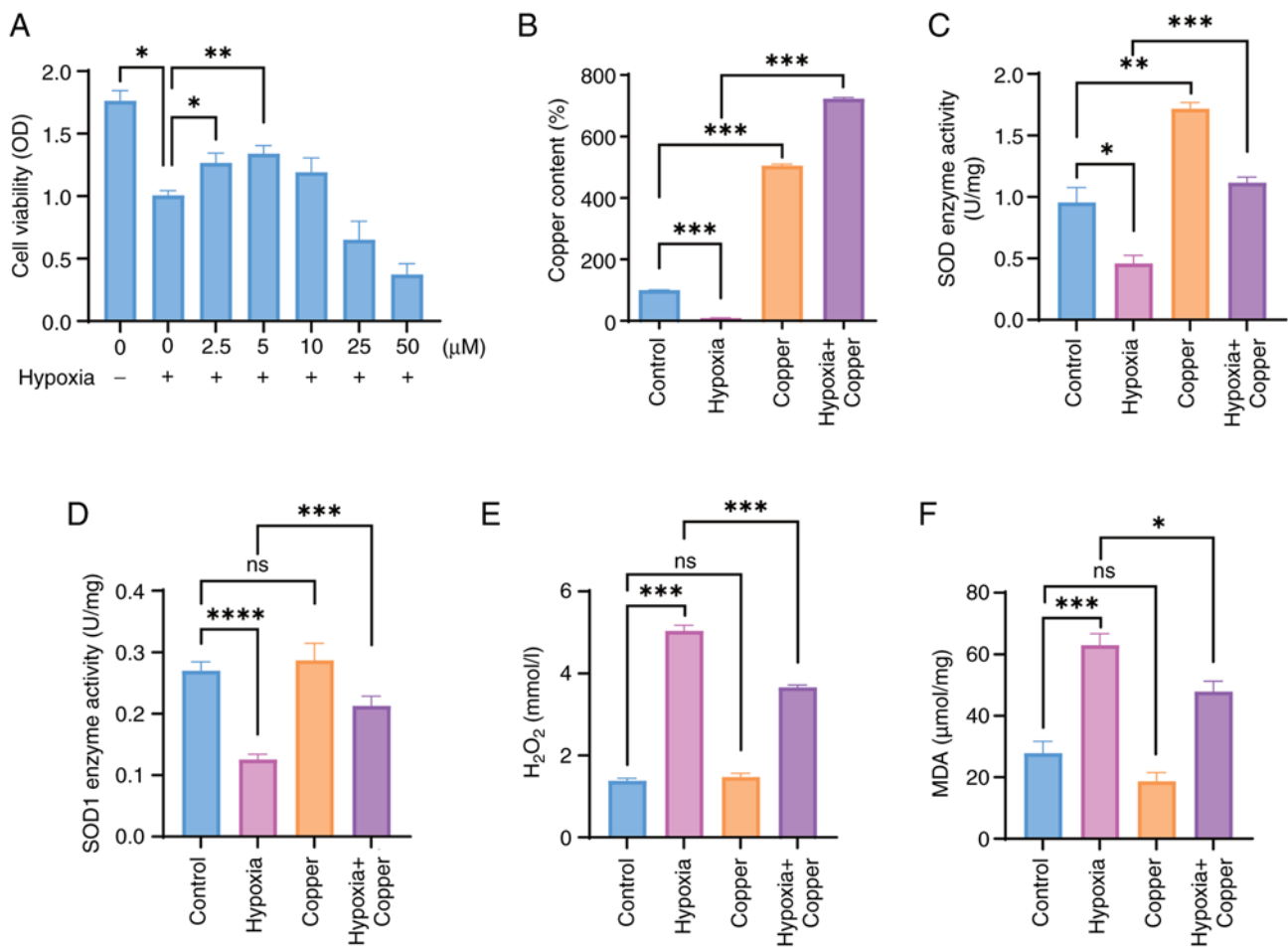


Figure 4. Copper can improve the viability of HT22 cells exposed to hypoxia through enhancing their anti-oxidative ability. (A) Viability of HT22 cells exposed to hypoxia (1% O₂) and different copper concentrations for 48 h, as detected by Cell Counting Kit-8 assay. (B) Copper content of HT22 cells after 48 h was detected by graphite furnace atomic absorption spectroscopy. (C) SOD and (D) SOD1 enzyme activity analysis. Detection of (E) H₂O₂ and (F) MDA in HT22 cells exposed to normoxia or hypoxia (1% O₂) for 48 h, with or without CuCl₂ (5 μM) exposure. One-way ANOVA was used for multiple-group comparisons. Data are presented as the mean ± SEM (n=3). *P<0.05, **P<0.01, ***P<0.001, ****P<0.0001. H₂O₂, hydrogen peroxide; OD, optical density; MDA, malondialdehyde; ns, not significant; SOD, superoxide dismutase.

Copper could improve the viability of HT22 cells exposed to hypoxia by enhancing their anti-oxidative ability. Based on the aforementioned experimental results, the present study assessed the effect of different concentrations of copper supplementation on the viability of HT22 cells after hypoxic exposure. Copper treatment after hypoxia resulted in a dose-dependent increase in cell viability when a dose ≤5 μM was administered (Fig. 4A); this suggested that an appropriate concentration of copper may promote the survival of cells exposed to hypoxia. Subsequently, the copper concentration in HT22 cells subjected to hypoxia and treated with 5 μM CuCl₂ was analyzed. The findings indicated a significant decrease in copper concentration in the hypoxia group compared with that in the control group, which is consistent with prior research (Fig. 3A). Conversely, HT22 cells exposed to hypoxia and treated with medium supplemented with 5 μM CuCl₂ exhibited elevated copper levels in comparison to the hypoxia group (Fig. 4B). The present study also examined the activities of SOD and SOD1 enzymes to investigate the potential of copper supplementation in mitigating oxidative stress induced by hypoxia. The results revealed a significant increase in SOD and SOD1

enzyme activity in HT22 cells in the hypoxia + copper treatment group compared with that in the hypoxia group (Fig. 4C and D). Moreover, H₂O₂ and MDA were examined, H₂O₂ and MDA levels were significantly decreased in the hypoxia + copper group compared with those in the hypoxia group (Fig. 4E and F). Overall, the present study indicated that an appropriate dose of copper may protect HT22 cells from hypoxia-induced oxidative stress.

Copper supplementation reduces hypoxia-induced ferroptosis. Given the decrease in copper concentration under hypoxic conditions, the present study investigated whether copper supplementation could alleviate hypoxia-induced ferroptosis and oxidative stress. First, the levels of intracellular ferrous ions were evaluated using a FerroOrange fluorescence probe. Despite the increase in intracellular ferrous ions in response to hypoxia, copper supplementation reduced the accumulation of intracellular ferrous ions under hypoxia, suggesting that copper may protect cells against ferroptosis (Fig. 5A and B). Next, the levels of LOS in HT22 cells exposed to hypoxia and treated with 5 μM copper were assessed, and it was revealed that the levels of LOS in the hypoxia + copper group were

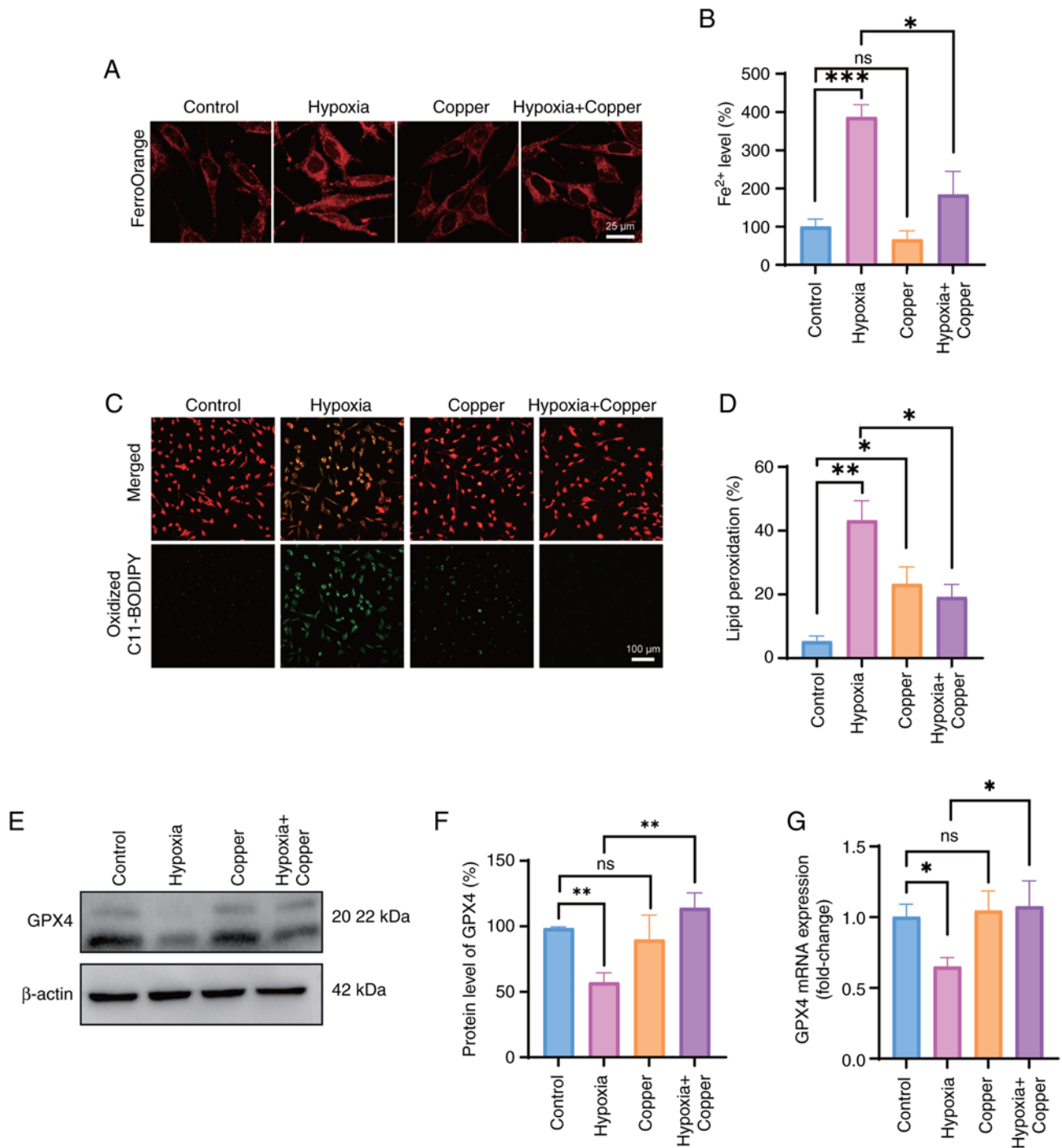


Figure 5. Copper protects neurons against ferroptosis induced by hypoxia. (A) Ferrous ion levels were detected by FerroOrange staining and (B) corresponding semi-quantification was performed using ImageJ. Scale bars, 25 μ m. (C) Lipid reactive oxygen species staining with the fluorescent probe C11-BODIPY and (D) corresponding semi-quantification. Scale bars, 100 μ m. (E) Western blot analysis and (F) semi-quantification of the protein expression levels of the ferroptosis biomarker GPX4 in HT22 cells exposed to normoxia or hypoxia (1% O₂) for 48 h, with or without CuCl₂ (5 μ M) exposure. (G) mRNA expression levels of GPX4 in HT22 cells exposed to normoxia or hypoxia (1% O₂) for 48 h, with or without CuCl₂ (5 μ M) exposure. One-way ANOVA was used for multiple-group comparisons. Data are presented as the mean \pm SEM (n=3). *P<0.05, **P<0.01, ***P<0.001. GPX4, glutathione peroxidase 4; ns, not significant.

significantly decreased compared with those in the hypoxia group (Fig. 5C and D).

Decreased GPX4 expression is notably associated with ferroptosis (21). Following the confirmation of hypoxia-induced ferroptosis in HT22 cells based on the aforementioned findings, an investigation was conducted to determine the effects of copper supplementation on ferroptosis. The effects of supplementation of the medium with 5 μ M CuCl₂ in the

hypoxia + copper group on GPX4 expression were examined. The expression levels of GPX4 in the hypoxia + copper group were significantly increased compared with those in the hypoxia group, indicating that copper supplementation may alleviate neuronal ferroptosis (Fig. 5E-G).

Copper alleviates hypoxia-induced neuronal injury through the CCS/SOD1/GPX4 axis. The present study analyzed the

expression of various copper-related proteins involved in cellular oxidative stress to examine the neuroprotective effects of copper in mitigating hypoxia-induced neuronal damage. Using a hypoxic model of HT22 cells supplemented with copper, western blot analysis revealed upregulation of XIAP expression, downregulation of CCS expression, and no significant change in the expression levels of SOD1 compared with those in the hypoxia group (Fig. 6A-D). Subsequently, siRNA targeting CCS was effectively transfected into cells (Fig. S2), followed by western blot analysis to assess the expression levels of CCS, SOD1 and GPX4 after exposure to hypoxia. Compared with in the hypoxia + Copper group, the protein expression levels of GPX4 were decreased in the hypoxia + Copper + siRNA group, whereas those of SOD1 remained significantly unchanged following siRNA knockdown of CCS (Fig. 6E-H). In addition, SOD1 activity and MDA content were detected after the knockdown of CCS (Fig. 6I-J). Consistent with the western blot analysis results, the rescue effects of copper supplementation after hypoxia were attenuated, as reflected by diminished increases in SOD1 enzyme activity and an increase in MDA content. In conclusion, the neuroprotective effects of copper may be mediated through the CCS/SOD1/GPX4 axis.

Discussion

The neuronal damage induced by hypoxia observed in the present study aligns with the findings reported in prior research that hypoxia could lead to neuronal oxidative stress and ferroptosis (22). The maintenance of central nervous system function requires appropriate levels of copper, as demonstrated by reports of impaired cognitive and motor functions in mammals with a copper deficiency (23). Studies have indicated a decrease in copper concentration in neurological disorders marked by hypoxia, suggesting the potential involvement of copper metabolism in the pathogenesis of hypoxia-induced neurological impairments (24,25). In the present study, a notable reduction in the copper concentration within neurons was observed following exposure to hypoxia. This decline in copper levels may contribute to the development of neurological impairment under hypoxic conditions, suggesting that copper could serve as a biomarker for brain damage induced by hypoxia.

Copper homeostasis mainly depends on the regulation of copper-related proteins, among which CTR1 is structurally and functionally conserved in humans, and is responsible for the majority of copper uptake into cells, whereas ATP7A and ATP7B act as major transporters for exporting copper from neurons (26,27). The expression levels of CTR1 were increased after exposure to hypoxia for 24 h but did not change after 48 h, which may be related to copper depletion in the cells. ATP7B expression was increased at 24 h but was significantly decreased at 48 h, which may be related to reduced cellular copper efflux after exposure to hypoxia for 48 h. The CCS chaperone facilitates the delivery of copper to SOD1 to detoxify ROS and maintain Cu homeostasis (28). It has been demonstrated that organisms deficient in SOD1 exhibit elevated oxidative stress levels (29). The present study observed a significant upregulation in CCS expression and a decrease in SOD1 enzyme activity following exposure to hypoxia. These changes were accompanied by increased

levels of oxidative stress markers, including ROS, H₂O₂ and MDA.

Oxidative stress resulting from hypoxia-induced injury is characterized by an excess of ROS, which can affect all neuronal cells (30). The present investigation detected elevated intracellular levels of ROS, H₂O₂ and MDA following exposure to hypoxia. SOD serves a crucial role in mitigating oxidative damage to tissues (31). The present findings indicated a significant decrease in SOD and SOD1 activity in HT22 cells subjected to hypoxic conditions, thus indicating that oxidative stress may have a critical role in neuronal injury following exposure to hypoxia.

Ferroptosis is a unique type of cell death resulting from iron accumulation and lipid peroxidation that can be blocked by Fer-1 (32). In the present study, ferroptosis was observed in neurons following hypoxia. It has previously been demonstrated that GPX4 is a key regulator of ferroptosis (33), and that the expression of GPX4 in neurons is significantly decreased after hypoxia. Additionally, the present study indicated a reduction in mitochondrial size, decreased mitochondrial ridges, increased bilayer membrane density, elevated levels of ferrous ions and lipid peroxidation in neuronal cells in response to hypoxia. The alterations in ferrous ions and lipid peroxidation were effectively reversed by Fer-1, which is consistent with the findings of a previous study (34).

In a prior study, treatment with copper was shown to reduce neuronal ferroptosis and oxidative stress (35). Notably, in the present study, the levels of H₂O₂ and MDA in the hypoxia + copper group were significantly reduced compared with those in the hypoxia group, indicating that copper can alleviate oxidative stress after hypoxic exposure. XIAP enhances E3 ubiquitination of the CCS by enhancing the delivery of copper to SOD1 to redistribute cellular copper and regulate copper homeostasis (36,37). SOD1 is a major antioxidant in cells, and copper is required for its maturation and enzymatic activity (38). The results of the current study indicated upregulation of XIAP protein expression and downregulation of CCS protein expression in response to copper supplementation in a hypoxic model, suggesting an increased requirement for copper in neurons under hypoxic conditions. Prior research has demonstrated the crucial role of the CCS in the antioxidant function of SOD1, as evidenced by a significant reduction in SOD1 activity in CCS-knockout mouse models (39,40). The present study also revealed that SOD1 activity was significantly reduced following CCS knockdown by siRNA without affecting its expression levels. Furthermore, GPX4 expression and MDA levels were comparable to those in the hypoxia group after copper treatment, suggesting that CCS/SOD1 may be involved in GPX4-mediated ferroptosis during neuronal hypoxic damage.

These findings indicated that copper could serve as a therapeutic agent for the prevention and treatment of hypoxic brain damage (41). Collective evidence has suggested that neuronal ferroptosis under hypoxic conditions may be attributable to disrupted copper metabolism and depletion. Further research, including *in vivo* studies and the elucidation of the precise mechanisms involved, is warranted to better understand the role of copper in ferroptosis following exposure to hypoxia.

In conclusion, exposure to hypoxia may disrupt copper metabolism, reduce copper levels in neurons, worsen oxidative stress and promote ferroptosis. Copper administration can help

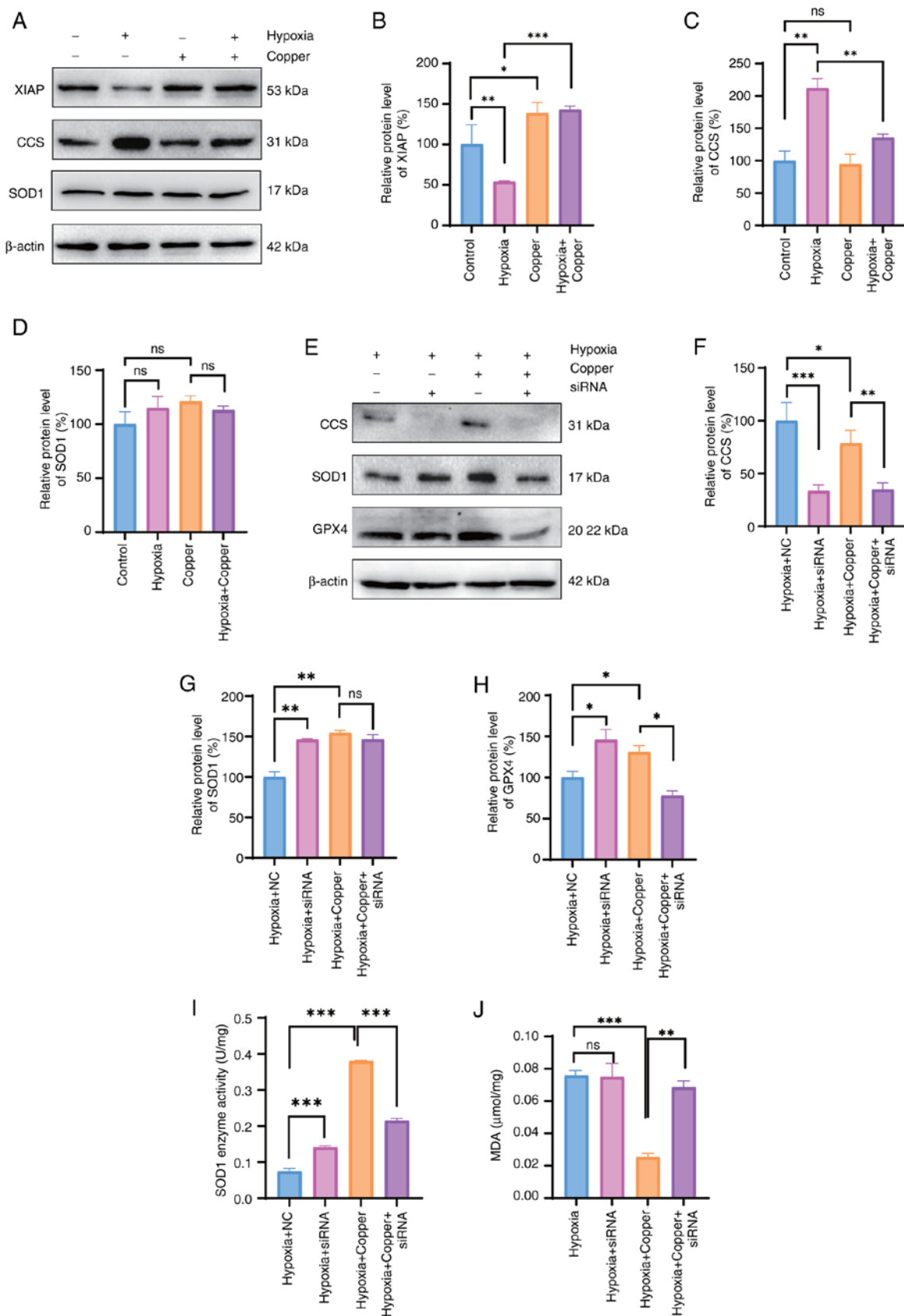


Figure 6. Copper alleviates hypoxia-induced neuronal injury through the CCS/SOD1/GPX4 axis. (A) Western blot analysis, and semi-quantification of the protein expression levels of copper transport proteins, including (B) XIAP, (C) CCS and (D) SOD1 following exposure to hypoxia (1% O₂) and copper supplementation for 48 h. (E) Western blot analysis, and semi-quantification of the protein expression levels of copper transport proteins, including (F) CCS, (G) SOD1 and (H) GPX4 was determined following exposure to hypoxia (1% O₂) for 48 h, with or without copper supplementation and CCS siRNA transfection. (I) SOD1 enzyme activity and (J) MDA content of HT22 cells following exposure to hypoxia (1% O₂) for 48 h, with or without copper supplementation and CCS siRNA transfection. One-way ANOVA was used for multiple-group comparisons. Data are presented as the mean \pm SEM (n=3). *P<0.05, **P<0.01, ***P<0.001. CCS, copper chaperone for superoxide dismutase; GPX4, glutathione peroxidase 4; MDA, malondialdehyde; NC, normal control; ns, not significant; siRNA, small interfering RNA; SOD1, superoxide dismutase 1.

alleviate oxidative stress and prevent neuronal ferroptosis, potentially serving as a therapeutic strategy for hypoxic brain damage.

Acknowledgements

The authors would like to thank Dr Weihua Yu (Fourth Military Medical University, Xi'an, China) for his suggestions and technical support for the laboratory experiments and data analysis.

Funding

This study was supported by the National Natural Science Foundation of China International Cooperation Program (grant no. 81920108030), the National Natural Science Foundation of China General Program (grant nos. 82271913, 82204089 and 82302116), the Fourth Military Medical University ZhuFeng project (grant no. 2020rcfczg), and the Air Force Medical University Pilotage Operation New Flight Program Project (grant no. 2023rcjfyk).

Availability of data and materials

The data generated in the present study may be requested from the corresponding author.

Authors' contributions

GZ, TW, JW and YZ conceived the study. ZZ and JW analyzed the data. ZC, RG, KJ, JW ST and LS developed the model and performed molecular biology experiments. RG was responsible for the supplementary work of the experiment. JW and RG confirm the authenticity of all the raw data. All authors read and approved the final version of the manuscript.

Ethics approval and consent to participate

Not applicable.

Patient consent for publication

Not applicable.

Competing interests

The authors declare that they have no competing interests.

References

- Douglas-Escobar M and Weiss MD: Hypoxic-ischemic encephalopathy: A review for the clinician. *JAMA Pediatr* 169: 397-403, 2015.
- Ahearne CE, Boylan GB and Murray DM: Short and long term prognosis in perinatal asphyxia: An update. *World J Clin Pediatr* 5: 67-74, 2016.
- Whitelaw A and Thoresen M: Therapeutic hypothermia for hypoxic-ischemic brain injury is more effective in newborn infants than in older patients: Review and hypotheses. *Ther Hypothermia Temp Manag* 13: 170-174, 2023.
- Golubnitschaja O, Yeghiazaryan K, Cebioglu M, Morelli M and Herrera-Marschitz M: Birth asphyxia as the major complication in newborns: Moving towards improved individual outcomes by prediction, targeted prevention and tailored medical care. *EPMA J* 2: 197-210, 2011.
- Arumugam TV, Baik SH, Balaganapathy P, Sobey CG, Mattson MP and Jo DG: Notch signaling and neuronal death in stroke. *Prog Neurobiol* 165-167: 103-116, 2018.
- Ji X, Zhou Y, Gao Q, He H, Wu Z, Feng B, Mei Y, Cheng Y, Zhou W, Chen Y and Xiong M: Functional reconstruction of the basal ganglia neural circuit by human striatal neurons in hypoxic-ischaemic injured brain. *Brain* 146: 612-628, 2023.
- Akyuva Y and Nazıroğlu M: Resveratrol attenuates hypoxia-induced neuronal cell death, inflammation and mitochondrial oxidative stress by modulation of TRPM2 channel. *Sci Rep* 10: 6449, 2020.
- Lin W, Zhang T, Zheng J, Zhou Y, Lin Z and Fu X: Ferroptosis is involved in hypoxic-ischemic brain damage in neonatal rats. *Neuroscience* 487: 131-142, 2022.
- Oorschot DE, Sizemore RJ and Amer AR: Treatment of neonatal hypoxic-ischemic encephalopathy with erythropoietin alone, and erythropoietin combined with hypothermia: History, current status, and future research. *Int J Mol Sci* 21: 1487, 2020.
- Davies KM, Hare DJ, Cottam V, Chen N, Hilgers L, Halliday G, Mercer JFB and Double KL: Localization of copper and copper transporters in the human brain. *Metallomics* 5: 43-51, 2013.
- Scheiber IF, Mercer JFB and Dringen R: Metabolism and functions of copper in brain. *Prog Neurobiol* 116: 33-57, 2014.
- Aleman S, Vilor-Tejedor N, Bustamante M, Álvarez-Pedrerol M, Rivas I, Fornis J, Querol X, Pujol J and Sunyer J: Interaction between airborne copper exposure and ATP7B polymorphisms on inattentiveness in scholar children. *Int J Hyg Environ Health* 220: 51-56, 2017.
- Zhang J, Cao J, Zhang H, Jiang C, Lin T, Zhou Z, Song Y, Li Y, Liu C, Liu L, *et al*: Plasma copper and the risk of first stroke in hypertensive patients: A nested case-control study. *Am J Clin Nutr* 110: 212-220, 2019.
- Zhang M, Li W, Wang Y, Wang T, Ma M and Tian C: Association between the change of serum copper and ischemic stroke: A systematic review and meta-analysis. *J Mol Neurosci* 70: 475-480, 2020.
- Gromadzka G, Tarnacka B, Flaga A and Adamczyk A: Copper dyshomeostasis in neurodegenerative diseases-therapeutic implications. *Int J Mol Sci* 21: 21239259, 2020.
- Yang S, Li X, Yan J, Jiang F, Fan X, Jin J, Zhang W, Zhong D and Li G: Disulfiram downregulates ferredoxin 1 to maintain copper homeostasis and inhibit inflammation in cerebral ischemia/reperfusion injury. *Sci Rep* 14: 15175, 2024.
- Sun X, Zhang X, Yan H, Wu H, Cao S, Zhao W, Dong T and Zhou A: Protective effect of curcumin on hepatolenticular degeneration through copper excretion and inhibition of ferroptosis. *Phytomedicine* 113: 154539, 2022.
- Li F, Wu X, Liu H, Liu M, Yue Z, Wu Z, Liu L and Li F: Copper depletion strongly enhances ferroptosis via mitochondrial perturbation and reduction in antioxidative mechanisms. *Antioxidants (Basel)* 11: 2084, 2022.
- Guan R, Yang C, Zhang J, Wang J, Chen R and Su P: Dehydroepiandrosterone alleviates hypoxia-induced learning and memory dysfunction by maintaining synaptic homeostasis. *CNS Neurosci Ther* 28: 1339-1350, 2022.
- Livak KJ and Schmittgen TD: Analysis of relative gene expression data using real-time quantitative PCR and the 2(-Delta Delta C(T)) method. *Methods* 25: 402-408, 2001.
- Yang WS, SriRamaratnam R, Welsch ME, Shimada K, Skouta R, Viswanathan VS, Cheah JH, Clemons PA, Shamji AF, Clish CB, *et al*: Regulation of ferroptotic cancer cell death by GPX4. *Cell* 156: 317-331, 2014.
- Zhu K, Zhu X, Liu S, Yu J, Wu S and Hei M: Glycyrrhizin attenuates hypoxic-ischemic brain damage by inhibiting ferroptosis and neuroinflammation in neonatal rats via the HMGB1/GPX4 pathway. *Oxid Med Cell Longev* 2022: 8438528, 2022.
- Bakraf N, Starr A, Rabichow BE, Lorenzini I, McEachin ZT, Kraft R, Chung M, Macklin-Isquierdo S, Wingfield T, Carhart B, *et al*: The M1311V variant of ATP7A is associated with impaired trafficking and copper homeostasis in models of motor neuron disease. *Neurobiol Dis* 149: 105228, 2021.
- Huuskonen MT, Tuo QZ, Loppi S, Dhungana H, Korhonen P, McInnes LE, Donnelly PS, Grubman A, Wojciechowski S, Lejavova K, *et al*: The Copper bis(thiosemicarbazone) complex Cu^{II}(atsm) is protective against cerebral ischemia through modulation of the inflammatory milieu. *Neurotherapeutics* 14: 519-532, 2017.
- Nikseresht S, Hilton JBW, Kysenius K, Liddell JR and Crouch PJ: Copper-ATSM as a treatment for ALS: Support from mutant SOD1 models and beyond. *Life (Basel)* 10: 271, 2020.

26. Chen L, Min J and Wang F: Copper homeostasis and cuproptosis in health and disease. *Signal Transduct Target Ther* 7: 378, 2022.
27. Batzios S, Tal G, DiStasio AT, Peng Y, Charalambous C, Nicolaides P, Kamsteeg EJ, Korman SH, Mandel H, Steinbach PJ, *et al*: Newly identified disorder of copper metabolism caused by variants in CTR1, a high-affinity copper transporter. *Hum Mol Genet* 31: 4121-4130, 2022.
28. Dong X, Zhang Z, Zhao J, Lei J, Chen Y, Li X, Chen H, Tian J, Zhang D, Liu C and Liu C: The rational design of specific SOD1 inhibitors via copper coordination and their application in ROS signaling research. *Chem Sci* 7: 6251-6262, 2016.
29. Fischer LR, Igoudjil A, Magrané J, Li Y, Hansen JM, Manfredi G and Glass JD: SOD1 targeted to the mitochondrial intermembrane space prevents motor neuropathy in the Sod1 knockout mouse. *Brain* 134: 196-209, 2011.
30. Meyer C, Rao NS, Vasanthi SS, Pereira B, Gage M, Putra M, Holtkamp C, Huss J and Thippeswamy T: Peripheral and central effects of NADPH oxidase inhibitor, mitoapocynin, in a rat model of diisopropylfluorophosphate (DFP) toxicity. *Front Cell Neurosci* 17: 1195843, 2023.
31. Borgstahl GEO and Oberley-Deegan RE: Superoxide dismutases (SODs) and SOD mimetics. *Antioxidants (Basel)* 7: 156, 2018.
32. Tang D, Chen X, Kang R and Kroemer G: Ferroptosis: Molecular mechanisms and health implications. *Cell Res* 31: 107-125, 2021.
33. Jiang X, Stockwell BR and Conrad M: Ferroptosis: Mechanisms, biology and role in disease. *Nat Rev Mol Cell Biol* 22: 266-282, 2021.
34. Doll S, Freitas FP, Shah R, Aldrovandi M, da Silva MC, Ingold I, Goya Grocin A, Xavier da Silva TN, Panzilius E, Scheel CH, *et al*: FSP1 is a glutathione-independent ferroptosis suppressor. *Nature* 575: 693-698, 2019.
35. Mezzaroba L, Alfieri DF, Colado Simão AN and Vissoci Reiche EM: The role of zinc, copper, manganese and iron in neurodegenerative diseases. *Neurotoxicology* 74: 230-241, 2019.
36. Wang L, Ge Y and Kang YJ: Featured article: Effect of copper on nuclear translocation of copper chaperone for superoxide dismutase-1. *Exp Biol Med (Maywood)* 241: 1483-1488, 2016.
37. Brady GF, Galbán S, Liu X, Basrur V, Gitlin JD, Elenitoba-Johnson KSJ, Wilson TE and Duckett CS: Regulation of the copper chaperone CCS by XIAP-mediated ubiquitination. *Mol Cell Biol* 30: 1923-1936, 2010.
38. Schmidt PJ, Kunst C and Culotta VC: Copper activation of superoxide dismutase 1 (SOD1) in vivo. Role for protein-protein interactions with the copper chaperone for SOD1. *J Biol Chem* 275: 33771-33776, 2000.
39. Wong PC, Waggoner D, Subramaniam JR, Tessarollo L, Bartnikas TB, Culotta VC, Price DL, Rothstein J and Gitlin JD: Copper chaperone for superoxide dismutase is essential to activate mammalian Cu/Zn superoxide dismutase. *Proc Natl Acad Sci USA* 97: 2886-2891, 2000.
40. Beckman JS, Esétvez AG, Barbeito L and Crow JP: CCS knockout mice establish an alternative source of copper for SOD in ALS. *Free Radic Biol Med* 33: 1433-1435, 2002.
41. Giampietro R, Spinelli F, Contino M and Colabufo NA: The pivotal role of copper in neurodegeneration: A new strategy for the therapy of neurodegenerative disorders. *Mol Pharm* 15: 808-820, 2018.



Copyright © 2024 Wang et al. This work is licensed under a Creative Commons Attribution-NonCommercial-NoDerivatives 4.0 International (CC BY-NC-ND 4.0) License.